ACS Catalysis

pubs.acs.org/acscatalysis Research Article

C−H Activation and Sequential Addition to Dienes and Imines: Synthesis of Amines with β-Quaternary Centers and Mechanistic Studies on the Complex Interplay Between the Catalyst and Three Reactants

Ramsey M. Goodner, Daniel S. Brandes, Gabriel N. Morais, Qiyuan Tao, Joseph P. Tassone, Brandon Q. Mercado, Shuming Chen,* and Jonathan A. Ellman*

Cite This: ACS Catal. 2024, 14, 18124−18133 Read Online

ACCESS | Metrics & More | Article Recommendations | Supporting Information

ABSTRACT: A Rh(III)-catalyzed sequential C−H bond addition to dienes and in situ formed aldimines was developed, allowing for the preparation of otherwise challenging to access amines with quaternary centers at the β-position. A broad range of dienes were effective inputs and installed a variety of aryl and alkyl substituents at the quaternary carbon site. Aryl and alkyl sulfonamide and carbamate nitrogen substituents were incorporated by using different formaldimine precursors. Moreover, the in situ formed *N*-Cbz aldimine from ethyl glyoxylate provided β,β-disubstituted α-amino esters with high diastereoselectivity. Two rhodacycle intermediates along the catalytic cycle were isolated and characterized by X-ray structural analysis, and the equilibria between the rhodacycle species in the presence of different reactants were determined. Deuterium labeling studies provided additional information to explain the uncommon 1,3-addition selectivity to the conjugated diene. Density functional theory calculations were consistent with the equilibria determined between the rhodacycle intermediates in the presence of different reactants and provided further insight on the transition state structures and energies for key steps in the catalytic cycle.

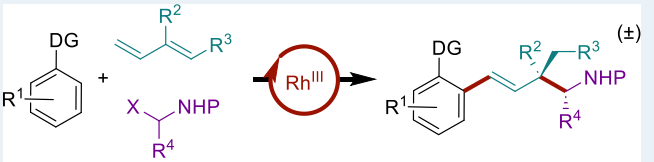

KEYWORDS: *homogeneous catalysis, C−H functionalization, C−C bond formation, aminomethylation, mechanism, rhodacycle*

INTRODUCTION

The transition metal-catalyzed sequential addition of C−H bonds to two different coupling partners is an efficient and modular way to introduce molecular complexity in a single step.[1] The Rh(III)- and Co(III)-catalyzed addition of C−H bonds to dienes and different types of electrophilic reactants, including aldehydes and ketones,[2,3] amidating,[4] cyanating,[5] and formylating reagents,[6] has proven to be a particularly powerful approach for the synthesis of diverse complex frameworks and often proceeds via an uncommon 1,3-addition to the diene (Scheme 1A). Notably, when internally substituted dienes are employed as reactants, a new bond forms at a challenging tetrasubstituted carbon site.

Amines are incorporated in a large majority of drugs and clinical candidates, thereby inspiring the development of transition metal-catalyzed additions of C−H bonds to imines (Scheme 1B). Several reports have appeared on C−H bond additions to activated imines such as *N*-Boc, *N*-tosyl, and *N*-*per*-fluorobutanesulfinyl derivatives [Scheme 1B(I)].[7] More recently, transition metal-catalyzed additions of arene C−H bonds to formaldimines have been explored to provide drug relevant aminomethylated products. For these applications, the high reactivity and poor stability of formaldimines has required that they be prepared in situ or be used as stock solutions [Scheme 1B(II)].[8]

Herein, we report the first examples of sequential C−H bond additions to dienes and highly reactive and unstable formaldimines, which posed a particular challenge for sequential addition because they needed to be generated in situ [Scheme 1C(1)]. Challenging quaternary centers were generated at the β-position to the amine using internally substituted dienes. A broad range of dienes were effective, including dienes with methyl, alkyl and aryl substituents at the R^2 position and hydrogen and aryl groups at the R^3 position. Moreover, different formaldimine precursors were employed to provide amine products protected with the tosyl, Cbz and Boc protecting groups. Given the frequency with which the sulfonamide motif occurs in drug structures, a variety of alkyl

Received: September 24, 2024
Revised: November 2, 2024
Accepted: November 15, 2024
Published: November 22, 2024

https://doi.org/10.1021/acscatal.4c05866
ACS Catal. 2024, 14, 18124−18133

Scheme 1. Sequential C−H Bond Addition to Dienes and Formaldimine Precursors

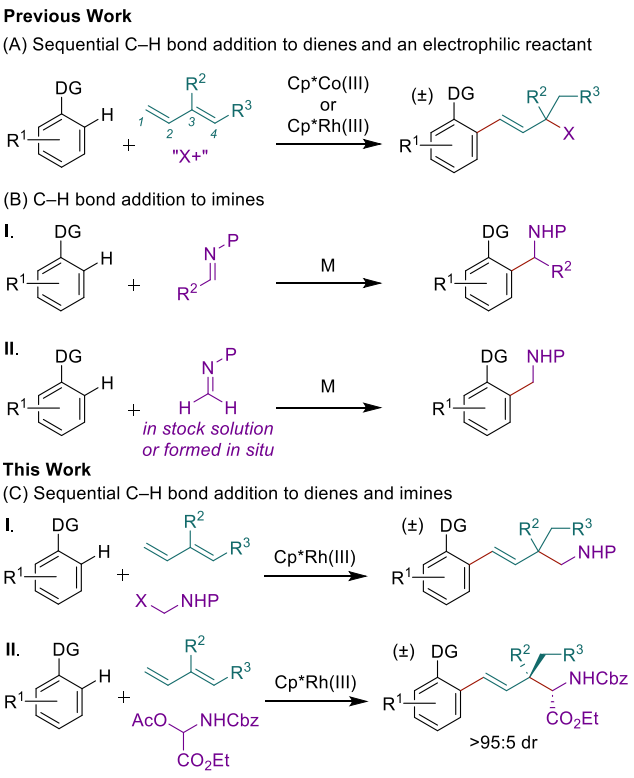

and aryl sulfonamide derivatives were also prepared. The in situ formed *N*-Cbz imine from ethyl glyoxylate also coupled with dienes incorporating different R^2 and R^3 substituents efficiently and with high diastereoselectivity to provide *β,β*-disubstituted *α*-amino esters that would be very difficult to access by other approaches [Scheme 1C(II)].

As represented by the reaction reported herein, the transition metal-catalyzed sequential addition of C−H bonds to two different coupling partners requires a complex interplay between the metal catalyst and three different reactants.[9] To elucidate the reaction mechanism, two new rhodacycle complexes along the catalytic cycle were isolated and characterized by X-ray structural analysis. Subjecting these rhodacycle intermediates to the reaction conditions in the presence of different reactants enabled the thermodynamic equilibrium between these species to be determined, and unexpectedly, established that product release from the catalyst requires the presence of both the C−H bond substrate and diene. DFT calculations were performed to provide further insight into the reaction mechanism and were consistent with the observed equilibria between rhodacycle intermediates. The observed equilibria and activation energies between the different species formed during the reaction have significant implications for the design of new C−H functionalization reactions with multiple coupling partners.

RESULTS AND DISCUSSION

Given Cui and co-workers' successful application of bis-(tosylamido)methane (BTM) for the direct aminomethylation of arene C−H bonds,[8b] we were motivated to first investigate BTM in our sequential C−H bond addition reaction. Extensive reaction optimization was conducted for the reaction of 2-(*m*-tolyl)pyridine (**1a**), isoprene (**2a**), and BTM (**3a**) (Table 1 and Tables S1−S3). The optimal conditions employed $[Cp^*RhCl_2]_2$ as the catalyst and sodium pivalate (NaOPiv) as a base additive with hexafluoroisopropanol (HFIP) as the solvent (entry 1). The Rh(III) catalyst was necessary for the reaction to occur (entry 2). Considering the 96% yield of the reaction under the standard conditions (entry 1), addition of the halide abstractor $AgB(C_6F_5)_4$ was not expected to provide any improvement (entry 3). However, when the basic 2-pyridyl directing group was substituted with less basic *N*-heterocycles, such as triazoles, the inclusion of the silver salt was required to obtain high yields (see Table S1). Other d^6 metal catalyst systems, such as $[Cp^*CoCl_2]_2$, $[Cp^*IrCl_2]_2$, and $[RuCl_2(p\text{-cymene})]_2$, did not provide appreciable product (entries 4−6, Table S2).

Table 1. Reaction Parameters for Sequential Addition

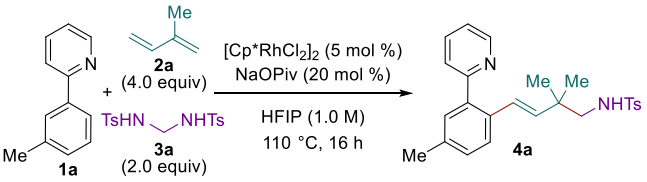

entry[a]	variation from standard conditions	yield 4a[b] (%)
1	none	96 (90)[c]
2	no $[Cp^*RhCl_2]_2$	0
3	$[Cp^*RhCl_2]_2$ (5 mol %), $AgB(C_6F_5)_4$ (20 mol %)	93
4	$[Cp^*CoCl_2]_2$ (5 mol %)	0
5	$[Cp^*IrCl_2]_2$ (5 mol %)	3
6	$[RuCl_2(p\text{-cymene})]_2$ (5 mol %)	0
7	no NaOPiv	86
8	NaOAc (20 mol %)	71
9	HOPiv (20 mol %)	65
10	1,4-dioxane as solvent	7
11	1,2-dichloroethane as solvent	10
12	toluene as solvent	14
13	toluene as solvent, $AgB(C_6F_5)_4$ (20 mol %)	62
14	90 °C	38
15	130 °C	63
16	0.5 M	65

[a]Conditions: Reactions were performed on 0.1 mmol of C−H bond substrate with 0.4 mmol of isoprene and 0.2 mmol of imine precursor. [b]Yields determined by ^1H NMR analysis with trimethylphenylsilane as a standard. [c]Isolated yield of pure material.

The addition of NaOPiv was not necessary when C−H bond reactants with the 2-pyridyl directing group were employed as substrates (entry 7), likely because the pyridine directing group is an effective base for C−H activation by concerted metalation deprotonation.[10] However, for less basic directing groups, NaOPiv resulted in improved yields, and thus was included in the standard reaction conditions (see Table S1). The use of the less hindered sodium acetate (entry 8) and pivalic acid (entry 9) as additives led to modest reductions in yield. HFIP proved to be the optimal solvent, and other common solvents for C−H activation reactions such as 1,4-dioxane, 1,2-dichloroethane, and toluene were much less effective (entries 10−12). Notably, when the chloride abstractor $AgB(C_6F_5)_4$ was added with toluene as the solvent, much of the conversion was restored (entry 13). These conditions were found to be optimal for the coupling of carbamate protected imine precursors (see Table S3).

Lowering the temperature from 110 to 90 °C provided a significant decrease in yield (entry 14), while raising the

https://doi.org/10.1021/acscatal.4c05866
ACS Catal. 2024, 14, 18124−18133

Scheme 2. Scope of Sequential C−H Addition to Dienes and Formaldimines[g]

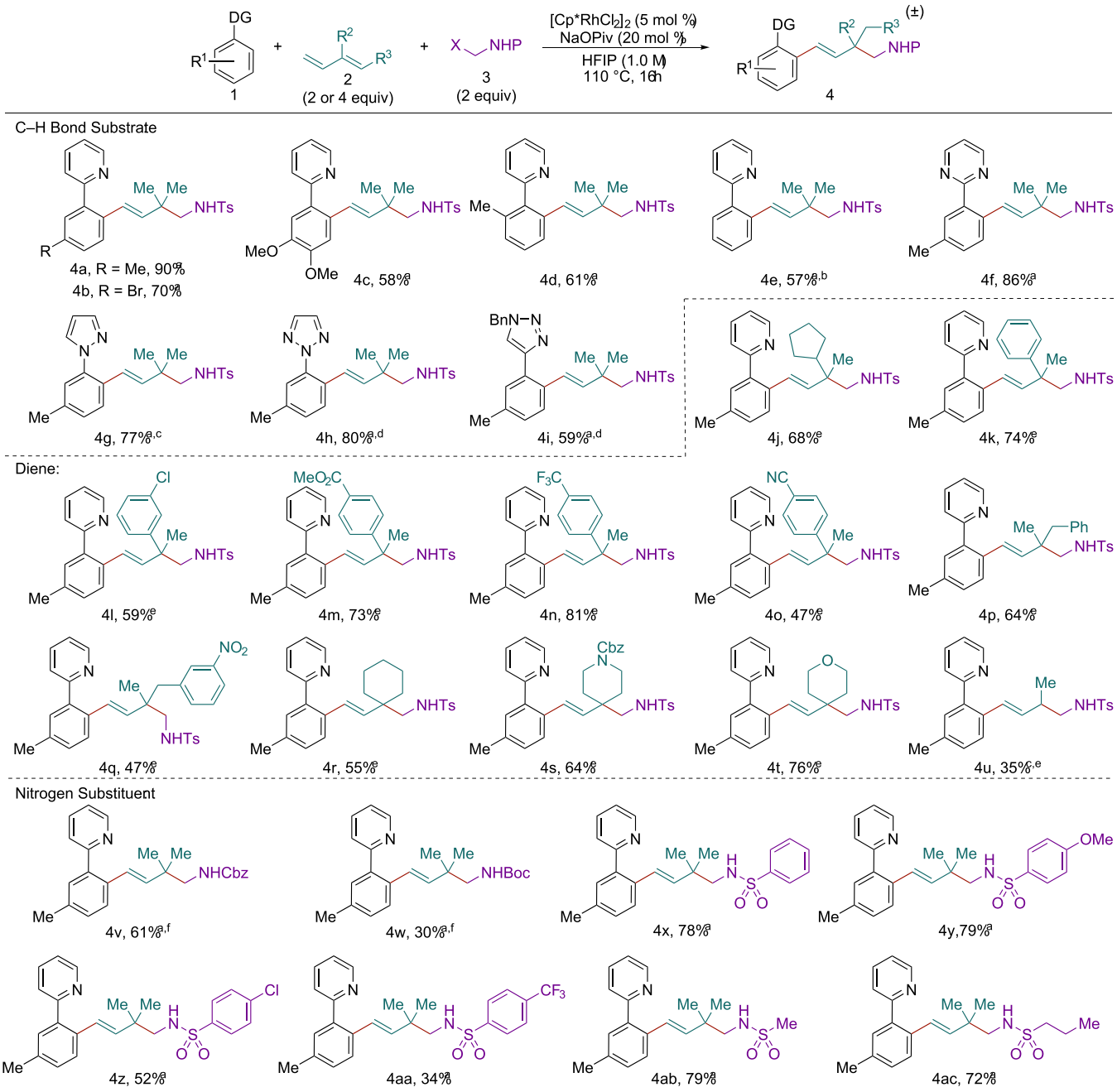

[a]Four equiv of diene. [b]Performed at 90 °C. [c]Performed at 130 °C. [d]Performed at 130 °C, 20 mol % of $AgB(C_6F_5)_4$. [e]Two equiv of diene. [f]X = OAc, Performed in toluene (1.0 M), 20 mol % of $AgB(C_6F_5)_4$. [g]X = NHP unless otherwise noted.

temperature to 130 °C gave a moderate drop to 63% yield (entry 15). However, for some substrates, lowering the temperature to 90 °C or raising the temperature to 130 °C was necessary to avoid formation of over addition products or enhance conversion to product, respectively (vide infra). Finally, when the concentration was halved from 1.0 to 0.5 M, the product was obtained in lower yield (entry 16).

After determining the optimal reaction conditions, we explored the scope of the C−H bond substrate, diene, and formaldimine precursor (Scheme 2). C−H bond substrates incorporating both electron donating and withdrawing *meta*-substituents were effective reactants (**4a** and **4b**). Moreover, the disubstituted bis-methoxyphenylpyridine could be employed (**4c**). In addition to *meta*-substituted 2-phenylpyridines, 2-(*o*-tolyl)pyridine was also an effective substrate in the sequential addition reaction to provide **4d** in 61% yield. For sterically unencumbered 2-phenylpyridine, the reaction temperature was lowered to 90 °C to minimize the formation of multicomponent products resulting from C−H activation at the unencumbered second *ortho* site of the product **4e**. In addition to substrates containing the 2-pyridyl directing group (**4a**−**4e**), other *N*-heterocyclic directing groups that are commonly found in drugs were also effective such as pyrimidine (**4f**), pyrazole (**4g**), and triazoles with different connectivity (**4h** and **4i**),[11] although a 130 °C reaction temperature or both the addition of $AgB(C_6F_5)_4$ and reaction

https://doi.org/10.1021/acscatal.4c05866
ACS Catal. 2024, 14, 18124−18133

at 130 °C proved necessary for the less basic pyrazole and triazole derivatives, respectively. Other directing groups, such as amides, were unsuccessful in the sequential addition reaction (see Chart S4 of the Supporting Information).

We next evaluated the diene scope and demonstrated that diverse 2-substituted and 1,2-disubstituted dienes were effective inputs. While 4 equiv of inexpensive isoprene had been employed under our optimal conditions, for the more substituted dienes we lowered the stoichiometry to 2 equiv given their decreased volatility. More sterically hindered 2-alkyl 1,3-dienes such as the branched 2-cyclopentyl butadiene coupled in good yield (**4j**). Importantly, 2-aryl butadienes with varied electronic profiles proved to be successful in the transformation (**4k**−**4o**). This reactivity contrasts with previously reported Rh(III)-catalyzed sequential additions of C−H bonds to dienes and aldehydes[2b] or amidating reagents[4] where only 1-aryl butadienes had been employed. Dienes with chloro (**4l**), methyl ester (**4m**), trifluoromethyl (**4n**), and cyano (**4o**) substituents were all effective inputs. However, electron-rich 2-aryl butadienes such as the *p*-methoxy derivative provided very poor conversion to the desired product, which was obtained in <10% yield (not shown).

Access to additional product classes could be achieved by utilizing 1,2-disubstituted dienes. For example, **4p** and **4q** were prepared from 1-aryl-2-methyl butadienes. Moreover, by employing 1-vinyl cycloalkenes, products incorporating cyclohexyl (**4r**), Cbz-protected piperidinyl (**4s**) and tetrahydropyranyl (**4t**) ring systems were all obtained. Lastly, the chemical feedstock butadiene was coupled in a modest though synthetically useful yield to provide the *β*-methyl amine **4u**, a structural motif found in bioactive compounds.[1] However, skipped dienes provided little if any sequential addition product under the standard reaction conditions (see Chart S4 of the Supporting Information).

We also explored the incorporation of a variety of nitrogen-substituents in addition to the *N*-toluenesulfonyl group. More readily cleaved carbamate protecting groups, including Cbz and Boc groups, could be installed using *N*,*O*-acetals[13] containing an acetate leaving group (**4v** and **4w**), although it was necessary to include the halide abstractor $AgB(C_6F_5)_4$ with toluene as the solvent.

Given that sulfonamides are found in many drugs,[14] we next evaluated *N*-sulfonyl formaldimine precursors to obtain products incorporating arenesulfonamides with different electronic properties as well as alkanesulfonamides. The parent benzenesulfonamide (**4x**) and electron-rich *p*-methoxybenzenesulfonamide (**4y**) products were obtained in high yield from the corresponding formaldimine precursors. However, the electron withdrawing *p*-chloro (**4z**) and *p*-trifluoromethyl (**4aa**) benzenesulfonamides were obtained in lower yield. Alkanesulfonamide imine precursors were also effective inputs providing **4ab** and **4ac** in good yields.

The reaction was further extended to the preparation of *β*,*β*-disubstituted *α*-amino esters by reaction of **3j**, a precursor to the *N*-Cbz imine from ethyl glyoxylate (Scheme 3).[15] By employing $AgB(C_6F_5)_4$ as a halide abstractor and toluene as the solvent, reaction with isoprene (**2a**) provided the *β*,*β*-dimethyl *α*-amino ester **4ad** in 48% yield. Three-component coupling with 2-aryl butadienes provided *α*-amino ester products **4ae**−**4ag** in 46−65% yields and with high diastereoselectivity (>95:5 dr). The relative stereochemistry of the methyl and ester groups in **4af** was rigorously determined by X-ray crystallographic analysis.[16] The 1,2-

Scheme 3. Sequential Addition to Dienes and Aldimines[a]

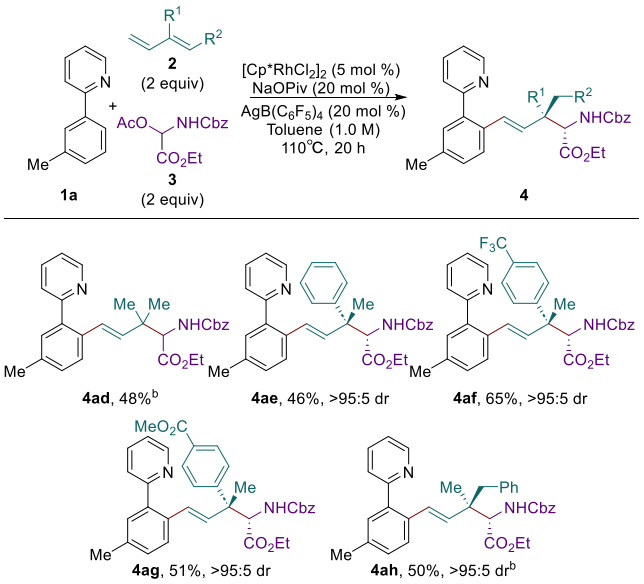

[a]Isolated yield of pure material. [b]Performed at 130 °C.

disubstituted diene **2h** also coupled with very high diastereoselectivity to give **4ah** with the opposite relative stereochemistry of the methyl and ester groups on the two contiguous stereogenic centers. The observed high stereoselectivity is consistent with the previously reported Co(III)-catalyzed sequential addition of C−H bonds to dienes and aldehydes, which also proceeds through a syn *β*-hydride elimination and reinsertion pathway (vide infra).[2c] The *β*,*β*-disubstituted *α*-amino esters, which were prepared in a single step using simple inputs, would be very difficult to synthesize by alternative approaches.

We conducted a preliminary exploration of asymmetric catalytic transformations (Scheme 4).[17] Only two examples of asymmetric catalytic Rh(III)-catalyzed C−H functionalization to install an acyclic quaternary center had previously been reported, and both relied on selective functionalization of enantiotopic methyl groups.[18] In contrast, for our sequential addition approach, face selective diene addition is required. After screening a variety of ligands and conditions (Tables S4−S6), we found that use of Cramer's elegantly designed Cp-ligand[19] **Rh1** led to promising selectivity in the catalytic enantioselective synthesis of *β*-quaternary amine products using both pyridyl (**4n**, **4ai**) and pyrazoyl (**4aj**, **4ak**) directing groups, as well as both sulfonamide (**4n**, **4aj**) and carbamate (**4ai**, **4ak**) nitrogen substituents. However, given the consistently low conversion to products **4**, we did not investigate the scope further.

Next, we conducted studies with isotopically labeled starting materials to aid in the elucidation of the mechanism for the sequential C−H bond addition to dienes and imines. When d_5-2-phenylpyridine (d_5-**1e**) was subjected to the standard reaction conditions for a truncated reaction time of 2 h at 90 °C, 57% of the C−H bond substrate was recovered (Scheme 5A). Spectroscopic analysis revealed 47% H/D exchange at the ortho positions, supporting a reversible C−H activation step.

Terminally dideuterated isoprene (d_2-**2a**) was also employed to investigate the selectivity for 1,3-disubstitution across the diene rather than the 1,2- or 1,4-addition patterns that are

https://doi.org/10.1021/acscatal.4c05866
ACS Catal. 2024, 14, 18124−18133

Scheme 4. Asymmetric Synthesis with Chiral Catalyst

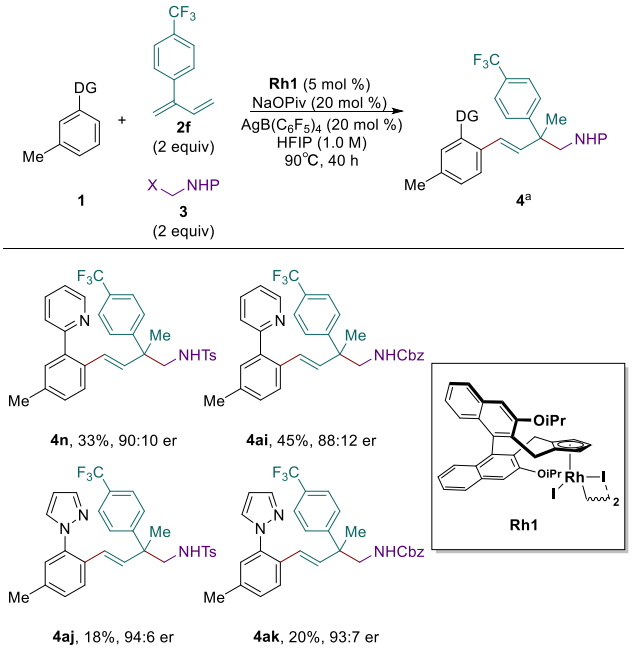

[a]Isolated yield of pure material.

Scheme 5. Deuterium Labeling Studies[a]

(A) Reaction with d_5-**1e** supports the reversibility of C–H activation

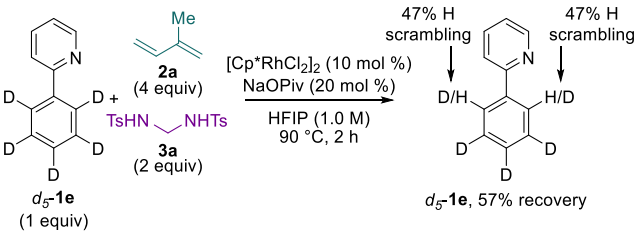

(B) Reaction of d_2-isoprene supports β-hydride elimination and reinsertion

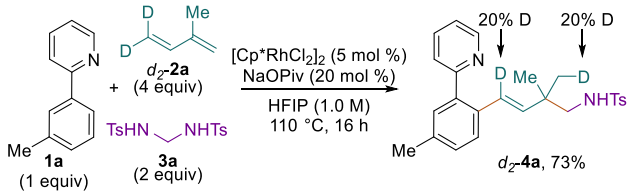

[a]Isolated yields of pure compounds reported.

typically observed for dienes (Scheme 5B).[4] Under the reaction conditions, deuterium migration was observed to one of the two methyl groups on the newly formed quaternary center in d_2-**4a**. This migration pattern is consistent with β-hydride elimination and reinsertion steps to give the observed 1,3-selectivity (vide infra) and contrasts with an allylic C–H activation step proposed for Rh(III)-catalyzed sequential C–H bond additions to dienes and aldehydes.[2b] Deuterium loss likely occurs by hydrogen–deuterium exchange from the Rh(III)-hydride intermediate, which is facilitated by the relatively acidic HFIP solvent (vide infra). It should be noted that when the reaction was performed in toluene in the absence of NaOPiv, less deuterium was lost (see Supporting Information, section V).

We also sought to further probe the reaction mechanism through the synthesis of hypothesized Rh(III)-intermediates along the catalytic cycle. For the previously reported Co(III)-catalyzed sequential C–H bond addition to butadiene and aldehydes, a cobalt–allyl complex was characterized by X-ray structural analysis and shown to serve as an intermediate along the catalytic cycle.[2a] To investigate the analogy of our Rh(III)-catalyzed transformation to the aforementioned Co(III)-catalyzed reaction, 2-(*m*-tolyl)pyridine (**1a**), isoprene (**2a**), stoichiometric amounts of $[Cp^*RhCl_2]_2$ and $AgB(C_6F_5)_4$ were heated in toluene resulting in isolation of the cationic Rh-allyl species **5a** (Scheme 6A).[16] X-ray structural characterization

Scheme 6. Isolation of Rh(III) Intermediates[a]

(A) Synthesis of rhodacycle **5a** via C–H addition into isoprene

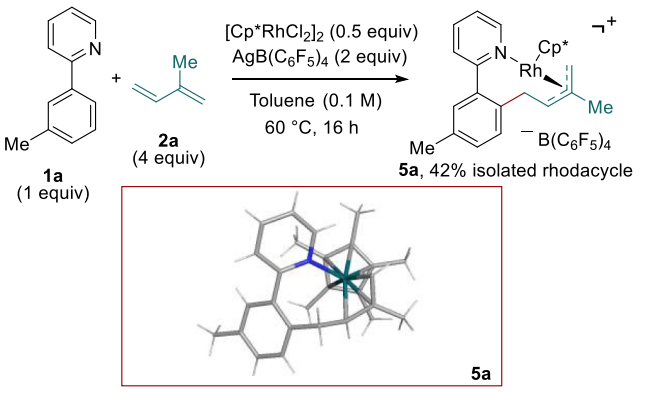

(B) Synthesis of rhodacycle **6** via reaction of **5a** and formaldimine precursors

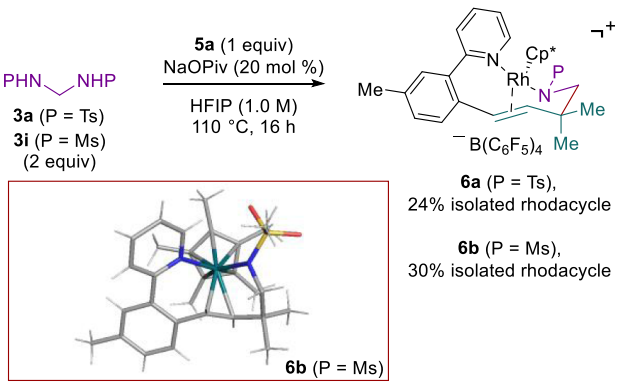

[a]Isolated yield of pure material.

revealed a saturated rhodium complex with η^3-allyl binding. To date, this is the first rhodacycle intermediate to be characterized by X-ray crystallography from a reaction of a Cp*Rh(III) catalyst, C–H bond reactant, and diene.

Rhodacycle **5a** was then reacted with a stoichiometric amount of BTM (**3a**) under the standard reaction conditions to provide a second rhodacycle **6a** corresponding to the 3-component sequential addition product still bound to the Cp*Rh(III) (Scheme 6B). Rhodium to alkene coupling was observed by ^{13}C NMR providing strong evidence for direct coordination of the alkene to rhodium (see Supporting Information, section XIII). Although we were not able to obtain X-ray quality crystals of product rhodacycle **6a**, the corresponding product rhodacycle **6b** with the smaller *N*-mesyl in place of the *N*-tosyl group in **6a**, readily formed crystals that were characterized by X-ray structural analysis.[16] The structure defined tridentate coordination to rhodium via the pyridine nitrogen, alkene, and deprotonated sulfonamide.

https://doi.org/10.1021/acscatal.4c05866
ACS Catal. 2024, 14, 18124–18133

To test the viability of rhodacycle **5a** as a reaction intermediate, 2-(*m*-tolylpyridine) (**1a**), isoprene (**2a**), and BTM (**3a**) were coupled in the presence of catalytic amounts of **5a** (Scheme 7A). The 87% yield obtained using rhodacycle

Scheme 7. Mechanistic Studies with Rh(III) Intermediates[a]

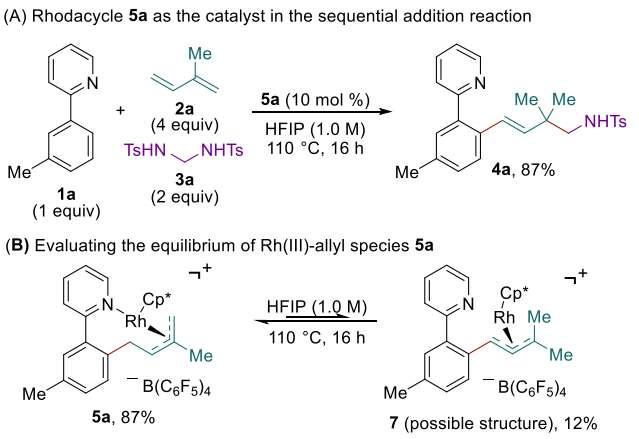

[a]Yields determined by ^{1}H NMR relative to trimethylphenylsilane as a standard.

5a as a catalyst was comparable to that observed under the optimized conditions with $[Cp^*RhCl_2]_2$ supporting rhodacycle **5a** as a competent intermediate along the catalytic cycle.

We were also interested in exploring the equilibrium between the two Rh(III)-allyl species along the proposed catalytic cycle (vide infra). Thus, we heated rhodacycle **5a** to 110 °C in HFIP overnight and obtained 87% recovery of allyl-complex **5a** (Scheme 7B). We also observed 12% of a new species by ^{1}H NMR, which we tentatively assign as Rh(III)-allyl complex **7**, a necessary intermediate for obtaining the observed product regioselectivity. However, we could not separate the newly formed species from the more stable rhodacycle **5a** to enable more rigorous structural characterization.

For C−H bond amidation and for additions to imines, mechanistic studies have established that amido-bound rhodacycles undergo concerted metalation-deprotonation with C−H bond substrates to complete the catalytic cycle and release the product.[10] We therefore hypothesized that release of the product **4a** from the product-bound rhodacycle **6a** could be accomplished in the presence of excess C−H bond substrate **1e** in HFIP with heating [Scheme 8A(I)]. To our surprise, we observed release of only 20% of the three-component product **4a** and only 11% of rhodacycle **8a** with much of the material remaining as product-bound rhodacycle **6a**. Presumably, poor conversion is due to an unfavorable equilibrium from the stable tridentate product-bound rhodacycle **6a** to product **4a** and the less stable bidentate rhodacycle **8a**. We therefore evaluated the reverse reaction by heating rhodacycle **8b** and product **4a** in HFIP and observed a high yield of product-bound rhodacycle **6a** along with two equivalents of 2-phenylpyridine (**1e**) [Scheme 8A(II)].

Based on the observed equilibration in the forward and reverse directions, we performed density functional theory (DFT) calculations to provide additional insight. Employing the *N*-mesyl rhodacycle **6b**, which we had also previously isolated (see Scheme 6B), the computed free energies show that 2-phenylpyridine and product-bound rhodacycle **6b** are 12.7 kcal/mol lower in energy than the product **4ab** and rhodium complex **8b** at 110 °C (Scheme 8A). These calculations are consistent with our experimental observation of minimal product release in the presence of C−H bond substrate alone. Taken together, these results raise the question of how catalyst turnover with release of product might be achieved under the reaction conditions.

To reconcile catalytic turnover despite the unfavorable equilibrium to product **4a** and rhodacycle **8**, product-bound rhodacycle **6a** was subjected to the reaction conditions in the presence of both 2-phenylpyridine (**1e**) and isoprene (Scheme 8B). Almost complete conversion to product **4a** and the stable η^3-allyl rhodacycle **5b** was observed with little remaining **6a**. Consistent with our experimental results, the calculated equilibrium between product-bound rhodacycle **6b**, 2-phenylpyridine and isoprene favored η^3-allyl rhodacycle **5b** and product **4ab** by −3.7 kcal/mol at 110 °C. Although the equilibrium between the C−H bond substrate and tridentate product-bound rhodacycle **6** to give the product **4** and bidentate rhodacycle **8** is unfavorable, with addition of isoprene, the overall equilibrium to the product **4** and η^3-allyl rhodacycle **5** is favorable due to the increased stability of this tridentate and coordinatively saturated species. In contrast, heating rhodacycle **6** in HFIP did not provide rhodacycle **5**, perhaps because this conversion would require release of an unstable formaldimine (see Section VIIf, Supporting Information).

Based on the studies with the isolated Rh(III) intermediates and isotope labeled starting materials, a mechanism is proposed as shown in Scheme 8C. To enter the catalytic cycle, reversible C−H activation by the Cp*Rh(III) catalyst via concerted metalation-deprotonation occurs, facilitated by an additional equivalent of C−H bond substrate with the 2-pyridyl directing group.[10] After coordination of the diene to **I**, migratory insertion into the terminal carbon of the diene occurs to form **II**. Intermediate **II** then undergoes reversible *syn*-β-hydride elimination and syn-reinsertion steps to yield a second, less stable η^3 Rh-allyl species **IV**. Imine addition via the chair transition state **V** then provides rhodacycle **VI**. Finally, the Rh-bound sequential addition product is released to give product **4** through ligand exchange with another molecule of C−H bond substrate to regenerate rhodacycle **I**, which upon addition to the diene provides the more stable tridentate rhodacycle **II**.

DFT calculations were conducted to provide a more complete picture of the relative energies of the Rh(III) intermediates throughout the full catalytic cycle with 2-(*m*-tolyl)pyridine (**1a**), isoprene (**2a**) and *N*-(methanesulfonamidomethyl)methanesulfonamide (**3h**) (Scheme 8D). Cationic rhodacycle **A** was set as the zero-point of the energy profile. After olefin coordination of diene **2a** to Rh(III) to give **B**, migratory insertion through **TS-1** with an energy barrier of 16.9 kcal/mol gives η^3-allyl rhodacycle **5a** in an overall exergonic event (−16.3 kcal/mol). From **5a**, an endergonic β-hydride elimination and reinsertion forms isomeric allyl rhodacycle **F** (−10.1 kcal/mol) by traversing **TS-2a** at 1.9 kcal/mol. Intermediate **5a** is lower in energy then the isomeric intermediates **D**, **E**, and **F**. These calculated relative energies are consistent with the formation of **5a** as a stable and isolable species (Scheme 6A), and our observation of minimal conversion of **5a** to other isomeric species under the reaction conditions (Scheme 7B). Interestingly, *syn*-β-hydride elimination from **5a** was calculated to have a

https://doi.org/10.1021/acscatal.4c05866
ACS Catal. 2024, 14, 18124−18133

Scheme 8. Mechanistic Investigation and DFT Calculations on the Relative Energy of Rh(III) Intermediates

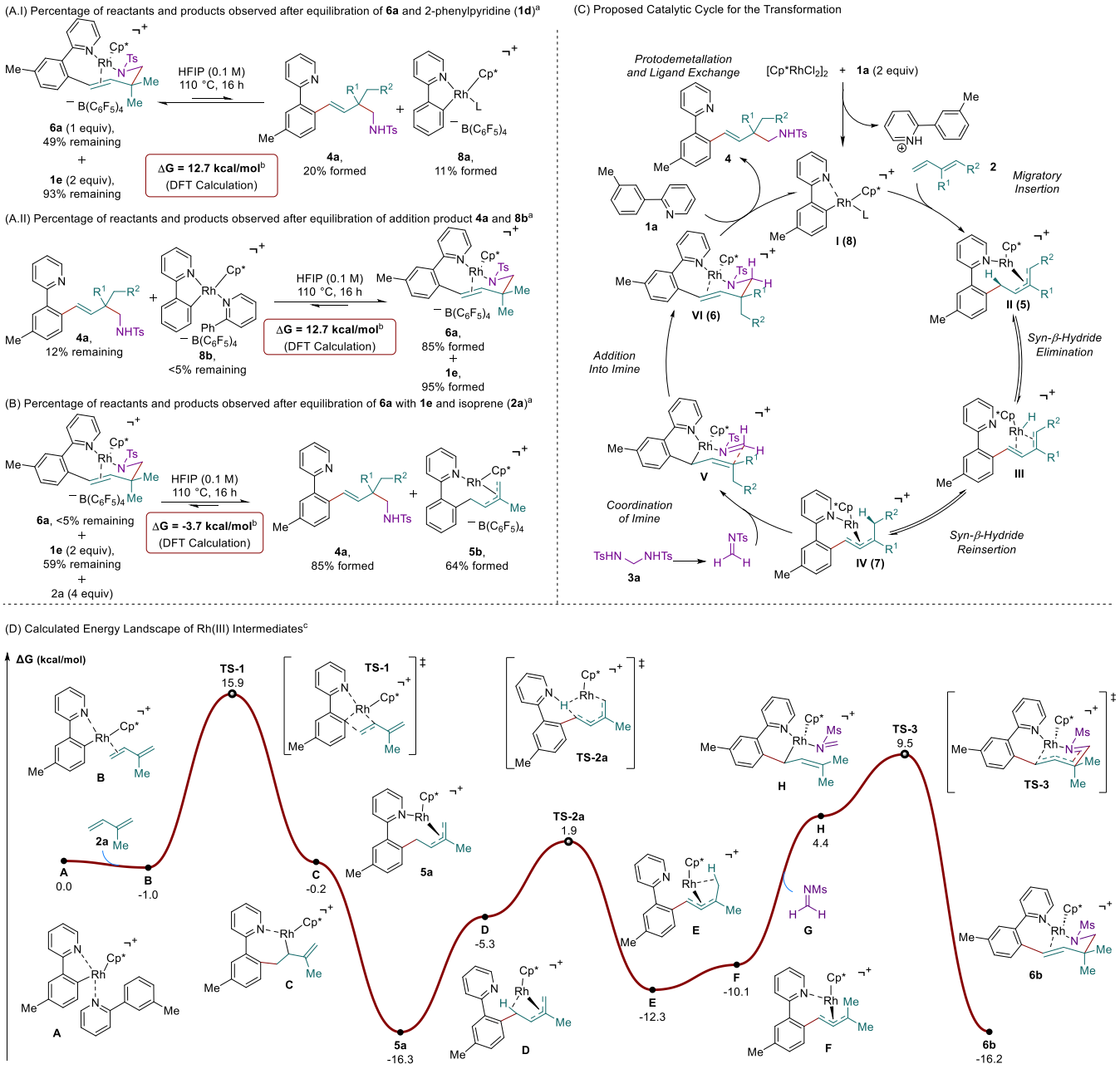

[a]Yields determined by ^{1}H NMR analysis with trimethylphenylsilane as a standard. [b]Calculated for NMs analog and for L = 2-phenylpyridine at 110 °C. [c]DFT calculations were performed at the M06-D3/def2-TZVPP−SDD(Rh), SMD(HFIP)//B3LYP-D3/def2-SVP−SDD(Rh) level of theory. Importantly, this reaction landscape shows only the relative energies of organometallic Rh(III) intermediates, which is in contrast to Scheme 8A,B where the overall free energy is calculated by accounting for all the species that are present.

significantly lower barrier (18.2−18.8 kcal/mol) when it is assisted by the pyridine moiety of the C−H bond substrate (see Supporting Information section XB). In contrast, the *syn*-*β*-hydride elimination barrier without pyridine assistance was calculated to exceed 30 kcal/mol. This result indicates that the directing group, as exemplified by the pyridyl group, can play a key role in facilitating the overall transformation beyond its function as the directing group for the C−H activation step.

Coordination of the Rh(III) center to in situ formed imine **G** (**H**, 4.4 kcal/mol) and addition into the imine through **TS-3** at 9.5 kcal/mol gives isolated rhodacyle intermediate **6b** (−16.2 kcal/mol). The highest kinetic barrier across the reaction landscape was calculated to be the overall conversion of rhodacycle **5a** to **6b**, which proceeded through **TS-3** with an overall $\Delta G^{\ddagger}$ of 25.8 kcal/mol, a magnitude consistent with the experimental observation that the reaction required elevated temperatures.

We also performed selected transformations of reaction products **4** (Scheme 9). First, Pd-catalyzed hydrogenation of the alkene in **4a** under acidic conditions provided **9**. Subjecting **4a** to strong acid promoted cyclization to the *N*-Ts protected pyrrolidine **10** in excellent yield. An in situ generated low valent titanium species was then employed to accomplish reductive cleavage of the *N*-tosyl group from **10** to provide the

https://doi.org/10.1021/acscatal.4c05866
ACS Catal. 2024, 14, 18124−18133

Scheme 9. Product Derivatizations[a]

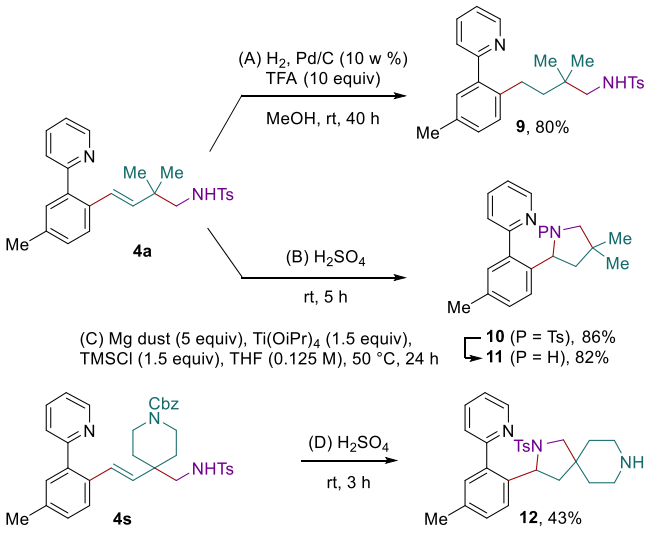

[a]Isolated yields of pure compounds reported.

free secondary amine **11** in good yield.[20] Treatment of cyclic product **4s** with H_2SO_4 resulted in concomitant cleavage of the Cbz group and cyclization to provide privileged spirocycle **12**, with the free piperidine nitrogen available for further elaboration.

CONCLUSIONS

In summary, we have reported the first sequential addition of arene C−H bonds to dienes and formaldimines formed in situ to obtain aminomethylated products with quaternary centers at the β-position. A broad scope was established for substituted dienes and formaldimine precursors. We further demonstrated coupling to the *N*-Cbz aldimine derived from ethyl glyoxylate to provide β,β-disubstituted α-amino esters with high diastereoselectivity. Thorough mechanistic studies were performed and included the isolation of new rhodacycle intermediates and investigation of key steps in the catalytic cycle to provide insight into the equilibria between these rhodacycle species and the three inputs in the reaction. DFT calculations supported these experimental observations and provided further insight on the transition state structures and energies for key steps in the catalytic cycle, including that the directing group plays a role beyond initial C−H activation. Collectively, these findings could have broad implications for the development of transition metal-catalyzed sequential C−H bond addition reactions as well as other multicomponent C−H functionalization reactions.

MATERIALS AND METHODS

All information pertaining to the materials and methods used in this study is provided in the Supporting Information.

ASSOCIATED CONTENT

Supporting Information

The Supporting Information is available free of charge at https://pubs.acs.org/doi/10.1021/acscatal.4c05866.

Experimental procedures; characterization data, NMR spectra, and crystallographic data for **4af**, **5a**, and **6b** (PDF)

Accession Codes

CCDC 2331084, 2331082, and 2331083 contain the supplementary crystallographic data for this paper. These data can be obtained free of charge via www.ccdc.cam.ac.uk/data_request/cif, or by emailing data_request@ccdc.cam.ac.uk, or by contacting The Cambridge Crystallographic Centre, 12 Union Road, Cambridge CB2 1EZ, UK; fax: +44 1223 336033.

AUTHOR INFORMATION

Corresponding Authors

Shuming Chen − *Department of Chemistry and Biochemistry, Oberlin College, Oberlin, Ohio 44074, United States;* orcid.org/0000-0003-1897-2249; Email: shuming.chen@oberlin.edu

Jonathan A. Ellman − *Department of Chemistry, Yale University, New Haven, Connecticut 06520, United States;* orcid.org/0000-0001-9320-5512; Email: jonathan.ellman@yale.edu

Authors

Ramsey M. Goodner − *Department of Chemistry, Yale University, New Haven, Connecticut 06520, United States*

Daniel S. Brandes − *Department of Chemistry, Yale University, New Haven, Connecticut 06520, United States;* orcid.org/0000-0003-2962-3175

Gabriel N. Morais − *Department of Chemistry and Biochemistry, Oberlin College, Oberlin, Ohio 44074, United States;* orcid.org/0000-0003-2439-8861

Qiyuan Tao − *Department of Chemistry, Yale University, New Haven, Connecticut 06520, United States*

Joseph P. Tassone − *Department of Chemistry, Yale University, New Haven, Connecticut 06520, United States*

Brandon Q. Mercado − *Department of Chemistry, Yale University, New Haven, Connecticut 06520, United States*

Complete contact information is available at: https://pubs.acs.org/10.1021/acscatal.4c05866

Author Contributions

The manuscript was written through contributions of all authors.

Notes

The authors declare no competing financial interest.

ACKNOWLEDGMENTS

The authors thank Dr. Fabian Menges (Yale) for assistance with mass spectrometry. This work was supported by NIH grant no. R35GM122473 (to J.A.E.). S.C. is grateful to the National Science Foundation (NSF CHE-2338438) and Oberlin College for financial support. DFT calculations were performed using the SCIURus, the Oberlin College HPC cluster (NSF MRI 1427949), as well as computing resources through allocation CHE210088 from the Advanced Cyberinfrastructure Coordination Ecosystem: Services & Support (ACCESS) program (NSF #2138259, #2138286, #2138307, #2137603, and #2138296).

REFERENCES

(1) Brandes, D. S.; Ellman, J. A. C−H bond activation and sequential addition to two different coupling partners: a versatile approach to molecular complexity. *Chem. Soc. Rev.* **2022**, *51*, 6738−6756.

(2) (a) Boerth, J. A.; Maity, S.; Williams, S. K.; Mercado, B. Q.; Ellman, J. A. Selective and synergistic cobalt(III)-catalysed three-component C−H bond addition to dienes and aldehydes. *Nat. Catal.* **2018**, *1*, 673−679. (b) Li, R.; Ju, C.-W.; Zhao, D. Rhodium(III) vs. cobalt(III): a mechanistically distinct three-component C−H bond addition cascade using a Cp*Rh^{III} catalyst. *Chem. Commun.* **2019**, *55*, 695−698. (c) Dongbang, S.; Shen, Z.; Ellman, J. A. Synthesis of Homoallylic Alcohols with Acyclic Quaternary Centers through Co^{III}-Catalyzed Three-Component C−H Bond Addition to Internally Substituted Dienes and Carbonyls. *Angew. Chem., Int. Ed.* **2019**, *58*, 12590−12594. (d) Shen, Z.; Li, C.; Mercado, B. Q.; Ellman, J. A. Cobalt(III)-Catalyzed Diastereoselective Three-Component C−H Bond Addition to Butadiene and Activated Ketones. *Synthesis* **2020**, *52*, 1239−1246.

(3) (a) Yang, J.; Ji, D.-W.; Hu, Y.-C.; Min, X.-T.; Zhou, X.; Chen, Q.-A. Cobalt-catalyzed hydroxymethylarylation of terpenes with formaldehyde and arenes. *Chem. Sci.* **2019**, *10*, 9560−9564. (b) Prusty, P.; Jeganmohan, M. Co(III)-Catalyzed three-component assembling of *N*-(2-pyrimidyl) indoles with dienes and formaldehyde. *Chem. Commun.* **2023**, *59*, 7216−7219. (c) Prusty, P.; Jeganmohan, M. Cobalt-catalyzed three-component assembly of aromatic oximes with substituted dienes and formaldehyde. *Chem. Commun.* **2024**, *60*, 10540−10543.

(4) (a) Pinkert, T.; Wegner, T.; Mondal, S.; Glorius, F. Intermolecular 1,4-Carboamination of Conjugated Dienes Enabled by Cp*Rh^{III}-Catalyzed C−H Activation. *Angew. Chem., Int. Ed.* **2019**, *58*, 15041−15045. (b) Mi, R.; Zhang, X.; Wang, J.; Chen, H.; Lan, Y.; Wang, F.; Li, X. Rhodium-Catalyzed Regio-Diastereo-and Enantioselective Three-Component Carboamination of Dienes via C−H Activation. *ACS Catal.* **2021**, *11*, 6692.

(5) Dongbang, S.; Ellman, J. A. Synthesis of Nitrile Bearing Acyclic Quaternary Centers through Co(III)-Catalyzed Sequential C−H Bond Addition to Dienes and *N*-Cyanosuccinimide. *Angew. Chem., Int. Ed.* **2021**, *60*, 2135−2139.

(6) Tassone, J. P.; Yeo, J.; Ellman, J. A. Three-component carboformylation: α-quaternary aldehyde synthesis *via* Co(III)-catalysed sequential C−H bond addition to dienes and acetic formic anhydride. *Chem. Sci.* **2022**, *13*, 14320−14326.

(7) (a) Tsai, A. S.; Tauchert, M. E.; Bergman, R. G.; Ellman, J. A. Rhodium(III)-Catalyzed Arylation of Boc-Imines via C−H Bond Functionalization. *J. Am. Chem. Soc.* **2011**, *133*, 1248−1250. (b) Li, Y.; Li, B.-J.; Wang, W.-H.; Huang, W.-P.; Zhang, X.; Chen, K.; Shi, Z.-J. Rhodium-Catalyzed Direct Addition of Aryl C−H Bonds to *N*-Sulfonyl Aldimines. *Angew. Chem., Int. Ed.* **2011**, *50*, 2115−2119. (c) Hesp, K. D.; Bergman, R. G.; Ellman, J. A. Rhodium Catalyzed Synthesis of Branched Amines by Direct Addition of Benzamides to Imines. *Org. Lett.* **2012**, *14*, 2304−2307. (d) Zhou, B.; Yang, Y.; Lin, S.; Li, Y. Rhodium-Catalyzed Direct Addition of Indoles to *N*-Sulfonylaldimines. *Adv. Synth. Catal.* **2013**, *355*, 360−364. (e) Yoshino, T.; Ikemoto, H.; Matsunaga, S.; Kanai, M. A Cationic High-Valent Cp*Co^{III} Complex for the Catalytic Generation of Nucleophilic Organometallic Species: Directed C−H Bond Activation. *Angew. Chem., Int. Ed.* **2013**, *52*, 2207−2211. (f) Yoshino, T.; Ikemoto, H.; Matsunaga, S.; Kanai, M. Cp*Co^{III}-Catalyzed C2-Selective Addition of Indoles to Imines. *Chem.—Eur. J.* **2013**, *19*, 9142−9146. (g) Parthasarathy, K.; Azcargorta, A. R.; Cheng, Y.; Bolm, C. Directed Additions of 2-Arylpyridines and Related Substrates to Cyclic Imines through Rhodium-Catalyzed C−H Functionalization. *Org. Lett.* **2014**, *16*, 2538−2541. (h) Wangweerawong, A.; Bergman, R. G.; Ellman, J. A. Asymmetric Synthesis of α-Branched Amines via Rh(III)-Catalyzed C−H Bond Functionalization. *J. Am. Chem. Soc.* **2014**, *136*, 8520−8523. (i) Boerth, J. A.; Hummel, J. R.; Ellman, J. A. Highly Stereoselective Cobalt(III)-Catalyzed Three-Component C−H Bond Addition Cascade. *Angew. Chem., Int. Ed.* **2016**, *55*, 12650−12654. (j) Xavier, T.; Rayapin, C.; Gall, E.; Presset, M. Multicomponent Aromatic and Benzylic Mannich Reactions through C−H Bond Activation. *Chem.—Eur. J.* **2019**, *25*, 13824−13828. (k) Cai, X.; Chen, W.; Nie, R.; Wang, J. Chiral-Directing-Group-Assisted Rhodium(III)-Catalyzed Asymmetric Addition of Inert Arene C−H Bond to Aldimines with Subsequent Intramolecular Cyclization. *Chem.—Eur. J.* **2021**, *27*, 16611−16615. (l) Lin, M.; Wu, Y.-F.; Liu, Z.-Q.; Liang, C.; Li, Q.-H.; Liu, T.-L. Rhodium(III)-catalyzed three-component C(sp^2)-H activation for the synthesis of amines. *Chem. Commun.* **2023**, *59*, 14431−14434.

(8) (a) Li, S.; Shi, P.; Liu, R.-H.; Hu, X.-H.; Loh, T.-P. Cobalt-Catalyzed N−O and C−C Bond Cleavage in 1,2-Oxazetidines: Solvent-Controlled C−H Aminomethylation and Hydroxymethylation of Heteroarenes. *Org. Lett.* **2019**, *21*, 1602−1606. (b) Li, Z.-Y.; Chaminda Lakmal, H. H.; Cui, X. Enabling Catalytic Arene C−H Amidomethylation via Bis(tosylamido)methane as a Sustainable Formaldimine Releaser. *Org. Lett.* **2019**, *21*, 3735−3740. (c) Ghosh, A. K.; Ghosh, P.; Hajra, A. Rhodium-Catalyzed Directed C(sp^2)−H Bond Addition of 2-Arylindazoles to *N*-Sulfonylformaldimines and Activated Aldehydes. *J. Org. Chem.* **2020**, *85*, 15752−15759.

(9) Whitehurst, W. G.; Kim, J.; Koenig, S. G.; Chirik, P. J. Three-Component Coupling of Arenes, Ethylene, and Alkynes Catalyzed by a Cationic Bis(phosphine) Cobalt Complex: Intercepting Metallacyclopentenes for C−H Functionalization. *J. Am. Chem. Soc.* **2022**, *144*, 4530−4540.

(10) (a) Tauchert, M. E.; Incarvito, C. D.; Rheingold, A. L.; Bergman, R. G.; Ellman, J. A. Mechanism of the Rhodium(III)-Catalyzed Arylation of Imines via C−H Bond Functionalization: Inhibition by Substrate. *J. Am. Chem. Soc.* **2012**, *134*, 1482−1485. (b) Li, Y.; Zhang, X.-S.; Li, H.; Wang, W.-H.; Chen, K.; Li, B.-J.; Shi, Z.-J. Mechanistic understanding of Rh-catalyzed *N*-sulfonylaldimine insertion into aryl C−H bonds. *Chem. Sci.* **2012**, *3*, 1634. (c) Park, S. H.; Kwak, J.; Shin, K.; Ryu, J.; Park, Y.; Chang, S. Mechanistic Studies of the Rhodium-Catalyzed Direct C−H Amination Reaction Using Azides as the Nitrogen Source. *J. Am. Chem. Soc.* **2014**, *136*, 2492−2502.

(11) (a) Guan, Q.; Xing, S.; Wang, L.; Zhu, J.; Guo, C.; Xu, C.; Zhao, Q.; Wu, Y.; Chen, Y.; Sun, H. Triazoles in Medicinal Chemistry: Physicochemical Properties, Bioisosterism, and Application. *J. Med. Chem.* **2024**, *67*, 7788−7824. (b) Marshall, C. M.; Federice, J. G.; Bell, C. N.; Cox, P. B.; Njardarson, J. T. An Update on the Nitrogen Heterocycle Compositions and Properties of U.S. FDA-Approved Pharmaceuticals (2013−2023). *J. Med. Chem.* **2024**, *67*, 11622−11655.

(12) (a) Ornstein, P. L.; Zimmerman, D. M.; Arnold, M. B.; Bleisch, T. J.; Cantrell, B.; Simon, R.; Zarrinmayeh, H.; Baker, S. R.; Gates, M.; Tizzano, J. P.; Bleakman, D.; Mandelzys, A.; Jarvie, K. R.; Ho, K.; Deverill, M.; Kamboj, R. K. Biarylpropylsulfonamides as Novel, Potent Potentiators of 2-Amino-3- (5-methyl-3-hydroxyisoxazol-4-yl)-propanoic Acid (AMPA) Receptors. *J. Med. Chem.* **2000**, *43*, 4354−4358. (b) Smith, B. M.; Smith, J. M.; Tsai, J. H.; Schultz, J. A.; Gilson, C. A.; Estrada, S. A.; Chen, R. R.; Park, D. M.; Prieto, E. B.; Gallardo, C. S.; Sengupta, D.; Dosa, P. I.; Covel, J. A.; Ren, A.; Webb, R. R.; Beeley, N. R. A.; Martin, M.; Morgan, M.; Espitia, S.; Saldana, H. R.; Bjenning, C.; Whelan, K. T.; Grottick, A. J.; Menzaghi, F.; Thomsen, W. J. Discovery and Structure-Activity Relationship of (1*R*)-8Chloro-2,3,4,5-tetrahydro-1-methyl-1*H*-3-benzazepine (Lorcaserin), a Selective Serotonin 5-HT_{2C} Receptor Agonist for the Treatment of Obesity. *J. Med. Chem.* **2008**, *51*, 305−313.

(13) (a) Harding, K. E.; Marman, T. H.; Nam, D. Stereoselective Synthesis of γ-hydroxy-α-amino acids via intramolecular amidomercuration. *Tetrahedron* **1988**, *44*, 5605−5614. (b) Fustero, S.; Jiménez, D.; Moscardó, J.; Catalán, S.; del Pozo, C. Enantioselective Organocatalytic Intramolecular Aza-Michael Reaction: a Concise Synthesis of (+)-Sedamine, (+)-Allosedamine, and (+)-Coniine. *Org. Lett.* **2007**, *9*, 5283−5286.

(14) Zhao, C.; Rakesh, K. P.; Ravidar, L.; Fang, W.-Y.; Qin, H.-L. Pharmaceutical and medicinal significance of sulfur (SVI)-Containing motifs for drug discovery: A critical review. *Eur. J. Med. Chem.* **2019**, *162*, 679−734.

(15) Roche, S. P.; Samanta, S. S.; Gosselin, M. M. J. Autocatalytic one pot orchestration for the synthesis of α-arylated, α-amino esters. *Chem. Commun.* **2014**, *50*, 2632−2634.

https://doi.org/10.1021/acscatal.4c05866
ACS Catal. 2024, 14, 18124−18133

(16) Deposition numbers 2331084 (major diastereomer of 4af), 2331082 (5a), and 2331083 (6b) contain the supplementary crystallographic data for this paper. These data are provided free of charge by the joint Cambridge Crystallographic Data Centre and Fachinformationszentrum Karlsruhe Access Structures service.
(17) For reviews, see: (a) Mas-Roselló, J.; Herraiz, A. G.; Audic, B.; Laverny, A.; Cramer, N. Chiral Cyclopentadienyl Ligands: Design, Syntheses, and Applications in Asymmetric Catalysis. *Angew. Chem., Int. Ed.* **2021**, *60*, 13198−13224. (b) Liu, C.-X.; Yin, S. Y.; Zhao, F.; Yang, H.; Feng, Z.; Gu, Q.; You, S. L. Rhodium-Catalyzed Asymmetric C−H Functionalization Reactions. *Chem. Rev.* **2023**, *123*, 10079−10134.
(18) (a) Kato, Y.; Lin, L.; Kojima, M.; Yoshino, T.; Matsunaga, S. Development of Pseudo-C_2-symmetric Chiral Binapthyl Monocarboxylic Acids for Enantioselective C(sp^3)−H Functionalization Reactions under Rh(III) Catalysis. *ACS Catal.* **2021**, *11* (7), 4271. (b) Shi, Y.; Qiao, Y.; Xie, P.; Tian, M.; Li, X.; Chang, J.; Liu, B. Rhodium-catalyzed enantioselective *in situ* C(sp^3)−H heteroarylation by a desymmetrization approach. *Chin. Chem. Lett.* **2024**, *35* (10), 109544.
(19) Ye, B.; Cramer, N. A Tunable Class of Chiral Cp Ligands for Enantioselective Rhodium(III)-Catalyzed C−H Allylations of Benzamides. *J. Am. Chem. Soc.* **2013**, *135*, 636−639.
(20) Shohji, N.; Kawaji, T.; Okamoto, S. Ti(O-*i*-Pr)$_4$/Me_3SiCl/Mg-Mediated Reductive Cleavage of Sulfonamides and Sulfonates to Amines and Alcohols. *Org. Lett.* **2011**, *13*, 2626−2629.

https://doi.org/10.1021/acscatal.4c05866
ACS Catal. 2024, 14, 18124−18133